Foundations and Reinforced Embankments
2A/1

Third International Conference on Geotextiles, 1986, Vienna, Austria

FLUET, J. E., Jr., GeoServices Inc., Consulting Engineers, USA
CHRISTOPHER, B. R., STS Consultants, Ltd., USA
SLATERS, A. R., Jr., Signode Corporation, USA

GEOSYNTHETIC STRESS-STRAIN RESPONSE UNDER EMBANKMENT LOADING CONDITIONS
CONTRAINTES ET DEFORMATIONS DANS UN GEOSYNTHETIQUE SOUS UN REMBLAI
SPANNUNGS-DEHNUNGS-VERHALTEN VON GEOSYNTHETICS IN EINEM DAMM

The paper describes a full scale test which models geosynthetically supported embankments constructed over subgrades which are expected to undergo a strength decrease with the passage of time. The test embankment was constructed on a geogrid spanning two support platforms separated by 4.7 m. The area between the platforms contained inflatable air bags which were used to simulate subgrades of various bearing capacities. The geogrid was fully instrumented for stress-strain response and deflection.

The test results verify a synergistic interaction between the embankment fill material and the suporting geogrid. The deflection of the test geogrid is compared in the paper to predictions by two analytical models, and relationships are presented which relate the actual test results to the model predictions.

Ein voller Massstab des Pruefungmodells geosynthetisher unterstuetzten Eindaemmung, konstruiert auf minderer Qualitaet, bei welcher es zu erwarten ist, dass sie sich mit der Zeit einer entkraeftigten Staerke unterzieht. Des Pruefungmodells Eindaemmung war auf einem Geogitter konstruiert und ist gespannft auf zwei gestuetzten Plattformen, geteilt durch 4.7 m. Die Flaeche zwischen den Plattformen beinhalten aufblasbare Luftpakete, welche gebraucht werden auf verschiedenen Traegerstaerken, um eine mindere Qualitaet zu simulieren. Das Geogitter wird voll angewendet fuer die Druckspannung auf deren Reaktion und Abweichung. Die Pruefungsresultate bestaetgen eine gegenseitige Wechselwirkung, welche zwischen der Eindaemmung gefuellten Material und den unterstuetzten Geogitter besteht. Die Abweichung des Geogitters ist verglichen mit der Vorhersage von zwei analytischen Modellen, deren Beziehung sich presentiert, welche die genauen Pruefungsresultate der Vorhersagung der Modelle betreffen.

1. INTRODUCTION

Numerous embankments incorporating geotextiles have been constructed on soils with very low shear strength (in some cases, <5 kPa). The design methods associated with such structures have been derived from a combination of experience, empirical evidence, and modifications of classical limit equilibrium analytical models [1]. In earlier research efforts, two subjects which have not been fully addressed are: (i) effects of soil-geosynthetic interaction; and (ii) stress-strain response and distribution within the geosynthetic.

This paper describes a full scale test embankment which was specifically designed and instrumented to evaluate soil-geosynthetic interaction as well as geosynthetic stress-strain response and distribution. A large quantity of data was generated, some of which is undergoing continuing analysis and will be presented in future papers.

2. BACKGROUND

Most current embankment design methods consider the following assumptions:

- No synergistic soil-geosynthetic interaction, i.e., the geosynthetic interacts with the soil just enough to mobilize its own tensile properties but not the mechanical properties of the soil or the soil-geosynthetic system. Accordingly, any imposed load not carried by the subgrade must be carried by the geosynthetic alone.
- Stress-strain response is uniform throughout the plane of the geosynthetic, i.e., the average load of the embankment is carried by the full width (Section A-A in Fig. 1) of the embankment, and no localized stress concentrations occur.

These assumptions may not always be conservative. For example, the development of significant soil-geosynthetic interaction would suggest that the resultant stresses in the geosynthetic would be lower than in the case where the geosynthetic acts alone. However, a more detailed analysis might show the opposite case to be true. In particular, the degree of interaction depends on soil properties which usually vary from location to location. The development of soil-geosynthetic interactive strength in one location may therefore result in a stress concentration in another location where no interaction occurs. This phenomenon may have occurred during this test and is discussed in more detail in Section 6.3.

These test results are particularly applicable to embankments constructed on subgrades whose strength is expected to decrease in the future. Examples are: karstic soils, frozen soils, and thermokarsts, (i.e., ice wedges and ice lenses). It should also be noted that, depending on soil properties, the degree of soil-geosynthetic interaction described herein is unlikely to occur if the depth of embankment covering material is less than approximately 1 m. Accordingly, this discussion is not applicable to thin embankments such as unpaved roads.

3. EMBANKMENT TEST MODEL

The test model consisted of a geosynthetically supported embankment spanning two support platforms located approximately 4.7 m apart. A conceptual drawing

of the experiment is shown in Fig. 1a, and the critical dimensions are shown in Figs. 1b and 1c. The 4.7 m between the edges of the support platforms is referred to herein as the "void". The "void" contained a pneumatically inflatable support system located beneath the geosynthetic and between the support platforms. The pneumatic support system consisted of nine disposable air bags connected by a fully variable manifold. By varying the air pressure, it was possible to simulate any subgrade bearing capacity from full support of the embankment to a void (0.0 kPa) (Fig. 1-c). It is recognized that the analogy to subgrade bearing capacity is not completely valid, i.e., any given subgrade soil may have deformation properties which differ from those of the pneumatic support system.

During construction of the final test, the embankment was supported by the pneumatic support system. The support system pressure was decreased in increments, and the stress transfer to the geosynthetic was monitored through instrumentation.

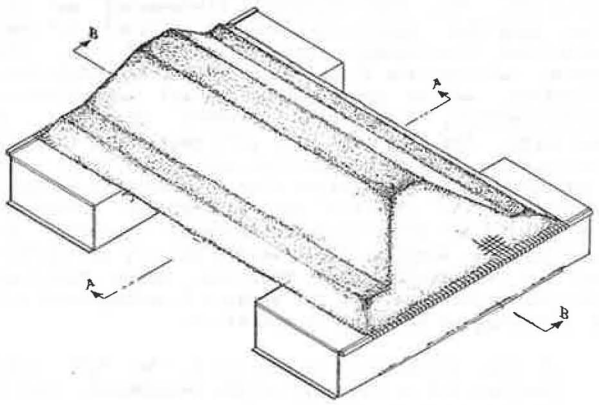

(a) Conceptual Drawing

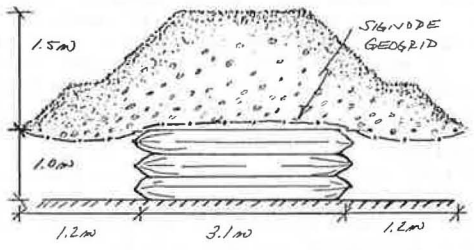

(b) Section A-A

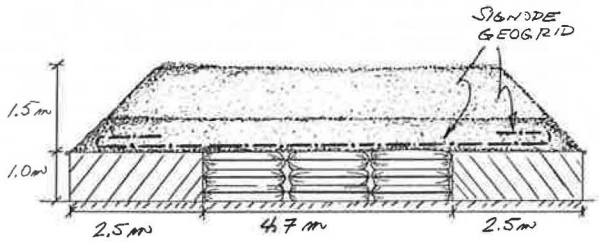

(c) Section B-B

Figure 1: Embankment Test Model

3.1 Geosynthetic Materials

The geosynthetic tested was a geogrid comprised of orthogonal strands of highly oriented polyester, each strand approximately 12 mm wide by 1mm thick, welded into a grid with nodes 40 mm by 50 mm on center. The geogrid has a wide strip tensile strength of 100 kN/m in the machine direction and 75 kN/m in the cross direction. Secant moduli in the machine direction are listed in Table A. All of the tensile properties were determined from wide width tensile tests using proposed ASTM 01.81.06, draft 9, procedures.

Table A: Geogrid Secant Moduli - Machine Direction

Elongation (%)	1	2	3	4	5
Secant Modulus (kN/m)	2190	1660	1450	1360	1300

3.2 Fill Material

The embankment fill material was a gravel with particle sizes from 2 mm to 40 mm, C_u = 2.5, unit weight of 17.35 kN/m^3, and friction angle of 42°. The fill was placed with a small backhoe and hand labor. Even though the holes in the grid were larger than all but the largest stones in the gravel, the interlock was sufficient to bridge the holes in the geogrid with minimum leakage. Only a small fraction of the gravel (2%) fell through the geogrid holes.

3.3 Procedure

The procedure for the final test was to:

- set up the support platforms and the pneumatic support system;
- inflate the pneumatic support system to provide a surface level with the platforms;
- place approximately 0.1 m of gravel on the platforms;
- place the geogrid;
- place approximately 0.3 m of gravel over the portions of the geogrid located over the platforms;
- wrap the remainder of the embedment geogrid around an anchor pipe and simultaneously remove any slack from the geogrid;
- place the remaining embedment geogrid over the gravel already placed;
- place an additional 1 m of gravel over the platform areas to anchor the geogrid;
- record initial readings from all instrumentation;
- place the gravel over the void area to a maximum height of 1.5 m, and continuously maintain the pneumatic support system at a pressure sufficient to provide full support (i.e., pressure in the pneumatic support system balances the pressure exerted by the gravel); and
- decrease the pneumatic support in 3.5 kPa increments, and record all data during each stabilization period (approximately 1 - 2 hours).

Prior to the conduct of the final test (using the above procedures) a test was run with no support from the pneumatic support system, i.e., the geogrid was allowed to deform as the gravel was placed. The actual tests were conducted under quite adverse weather conditions (wind and intermittent rain).

3.4 Instrumentation

In order to determine the strains in the geogrid in both principal directions, strain gauges were placed at

locations indicated in Fig. 2. A multichannel data acquisition system was used to monitor and record the data. Three types of gauges were utilized:

- Micro-Measurements Group, Inc. bonded resistance foil strain gauges Type EP-08-250BG-120 were used as the primary strain measurement gauge. These gauges were epoxied directly onto the top and bottom of individual strands of the geogrid in the proper orientation.

- As a backup to the bonded resistance gauges, several electro-magnetic inductance type soil strain gauges (Bison Model 4101-A) were incorporated into the instrumentation arrangement and located near the bonded resistance gauges. These disc-shaped coil strain gauges were placed in co-axial alignment with each other on the strand over which the strain was to be measured. By placing three gauges at each location, strains could be measured in each principal direction. The gauges were affixed to the underside of the geogrid so that they would not be damaged by gravel.

- To complement the two types of electrical strain gauges, mechanical wire extensometers were attached to the geogrid in pairs at locations indicated on Fig. 2. The gauge spacing varied so that differential strain over large distances could be measured. The wire gauges were fed through plastic tubing so that friction would be reduced through the gravel embankment.

In addition to the above strain gauge instrumentation, a survey was performed by placing stand pipes within the gravel along the centerline of the embankment. A survey of the pipe elevations was performed at each pressure reduction interval to evaluate total deformation of the system. The pressure

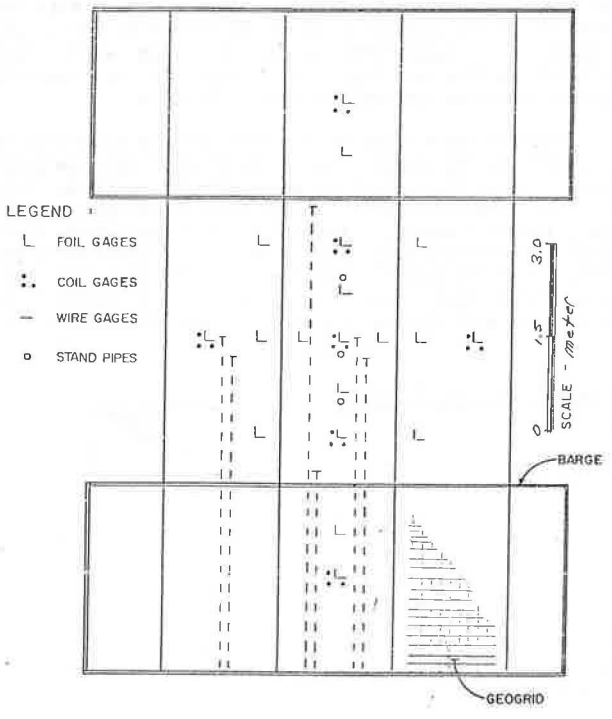

Figure 2: Location of Instrumentation Devices

in the pneumatic support system was determined through a system of pressure gauges, and maintained at desired levels through a baffle arrangement.

Initial readings were obtained after all of the gravel was loaded onto the geogrid and was fully supported by the pneumatic support system. Readings were then obtained after each pressure decrease until the pneumatic system pressure was zero. Through instrumentation, it was possible to monitor: (i) geosynthetic strain at various locations; (ii) gravel thickness and load distribution; (iii) vertical deflection of the geosynthetic; and (iv) pressure in the inflatable "subgrade".

4. INITIAL ANALYTICAL EVALUATION

The test was modeled using two different analytical approaches: one assuming no soil-geogrid interlock and full support by the geogrid alone, and the other assuming strong interlock and a beam-like response corresponding to support by a synergistically acting soil-geogrid system.

4.1 Fully Flexible Model

This model is based on Kinney [2] and assumes that the geogrid and/or the subgrade provided the only support to the embankment load (i.e., no benefit from soil-geogrid interaction). As a further simplification, it is assumed that the resultant normal stress on the geogrid is due to the weight of the embankment minus the subgrade support. Whereas this assumption is approximately true as an average, at any given moment the actual subgrade support conditions probably vary from zero to more than the measured gauge pressure. This latter effect is due to the ballooning of the pneumatic support system, i.e., loss of contact at the edges of the airbags with increasing inflation.

The fully flexible model parameters are shown schematically in Fig. 3, where: $T = qr$; $W = 2r \sin\theta$; $E = T/\tau$; $D = r - r\cos\theta$; and $\tau = 2\,q \tan\phi_{SG}$.

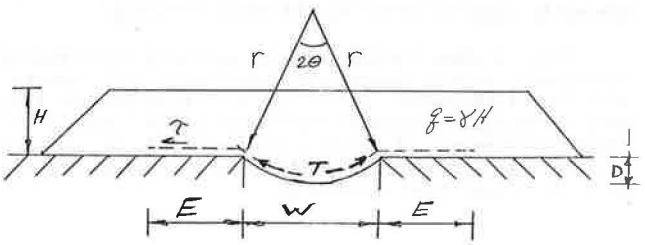

Figure 3. Fully Flexible Model Parameters

4.2 Full Interlock Model

Another method of analysis is to assume that the system acts like a beam. In this concept, the geogrid and the gravel are assumed to act integrally as a reinforced geogrid-gravel "beam" which spans over the space intervening between the two support platforms. Tension is assumed to be carried by the geogrid and compression by the gravel. It is assumed that no slip occurs between the gravel and the grid. The analysis is made using the analogy of a reinforced concrete beam designed for its ultimate stregth. Fig. 4 describes the parameters and calculations used, where: M_u = ultimate

moment capacity; d = equivalent rectangular beam depth; F_t = tensile strength of geogrid; A_g = area of geogrid; F_{yg} = yield strength of geogrid; and F_c = compressive strength of gravel.

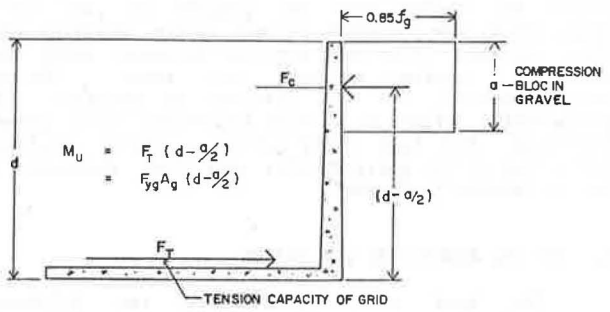

Figure 4: Full Interlock Model Parameters

5. RESULTS

Two tests were performed. In the first test, the embankment was constructed without pneumatic support beneath the embankment in the void area. As a result, after placement of 1.2 m of gravel on the system, the system reached maximum deflection (0.8 m).

The second test was constructed to the full embankment height (1.5 m) over the inflated pneumatic support system. The full embankment height was maintained as the support pressure was decreased from 26 kPa (which provided full support since 26 kN/m^2 = 17.35 kN/m^3 x 1.5 m) to 0.0 kPa. Under zero pneumatic support, the soil-geogrid system was found to fully support the embankment. The system subsequently creeped to failure in approximately 2 hours.

Fig. 5 presents the vertical settlement profile versus the support pressure in the pneumatic support system. The data shows a maximum vertical deformation of 0.6 meters under the fully loaded condition (no pneumatic support) prior to the onset of creep.

Fig. 6 shows typical results measured using bonded resistance strain gauges and inductance coil gauges. Wireline extensometer results are not shown because they were principally used as individual point sources to check performance of electrical gauges and to correct overall strain information for slack in the geogrid prior to actual load application.

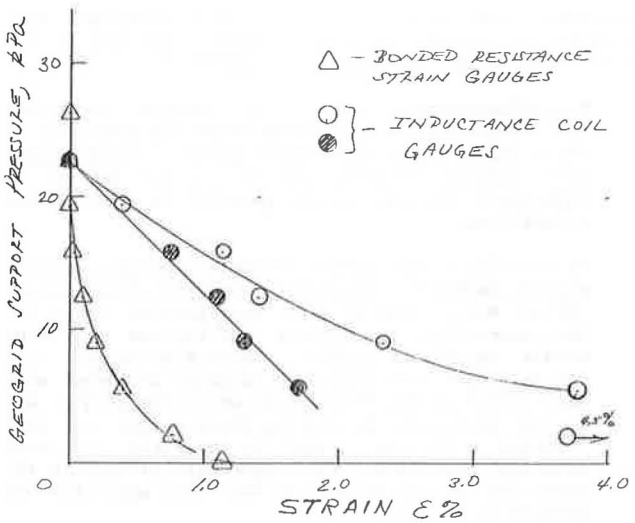

Figure 6: Typical Strain Data, Measured at Various Locations on Geogrid.

6. DISCUSSION OF RESULTS

6.1 Soil-Geogrid Interaction

Perhaps the most notable results were the clear indications of soil-geogrid synergism. This effect was demonstrated in several ways. A vivid demonstration is shown by comparing Figs. 7a and 7b. In Fig. 7a, the geogrid was loaded without any pneumatic support and allowed to deform as the load was increased. In Fig. 7b, the same geogrid was fully supported by the pneumatic system until all of the load had been placed, and then was allowed to deform. In Fig. 7b, with the pressure of the pneumatic system decreased to zero, the geogrid is supporting a heavier load with less deformation than in Fig. 7a, i.e., the soil-geogrid system is acting synergistically in Fig. 7b.

Another indication of the soil-geogrid synergism is provided by the progressive deflection of the geogrid. Table B shows the actual maximum deflections (from Fig. 5) in comparison to the deflections predicted by the fully flexible model. Table B shows actual deflections which are considerably lower than those predicted by the fully flexible model. It is noteworthy that the non-interactive test shown in Fig. 7a did deflect in accordance with the fully flexible model (Section 4.1).

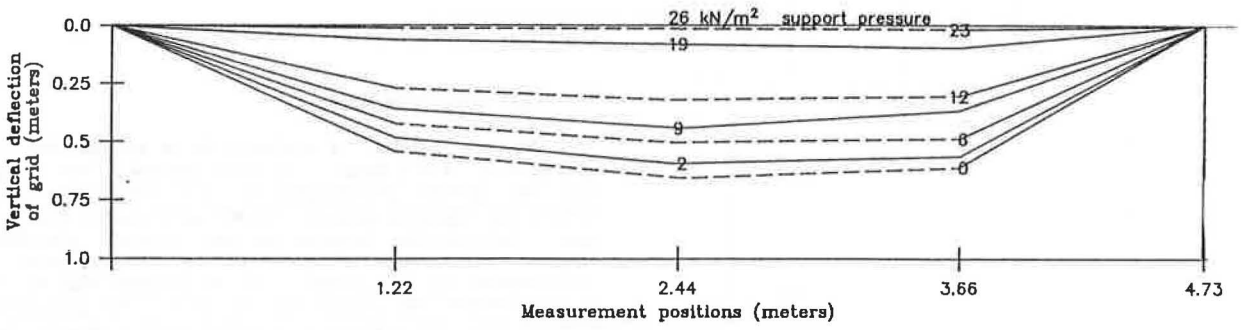

Figure 5: Vertical Settlement Profile of Embankment

There appears, at least in this test, to exist a linear relationship between the actual interactive deflection (D_{act}) and the deflections predicted by the fully flexible model (D_{mod}). Specifically,

$$D_{act} = 1.24\ D_{mod} - 0.50 \quad (D_{act},\ D_{mod} \text{ in m})$$

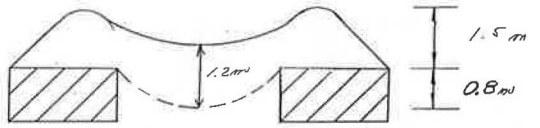

(a) fully flexible deformation (without support)

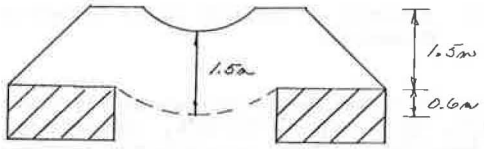

(b) soil-geogrid interactive deformation (with support)

Figure 7. Final Profiles With and Without Pneumatic Support During Initial Loading

Table B: Actual versus Flexible Model Deflections

Support System Pressure (kPa)	Assumed Normal Stress* (kPa)	Flexible Model D_{mod} (m)	Actual D_{act} (m)
23	3	0.40	0.02
19	7	0.50	0.08
13	13	0.65	0.32
9	17	0.74	0.44
6	20	0.81	0.50
2	24	0.89	0.59
0	26	0.92	0.60

* Equals stress from embankment gravity stress (26 kPa) minus support system pressure

Other investigators who have similar data may wish to see if this relationship has broader application. At least part of the soil-geogrid interaction appears to be the promotion of arching within the soil mass. This phenomenon is shown schematically in Fig. 8. As shown in the figure, the soil in the shaded area is supported, through arching, from outside the void area even though the soil is physically located over the void area. This phenomenon relies not only on the presence of the geogrid, but also on the development of the interactive process. In this specific case, a 1.5 m high gravel embankment could not mobilize sufficient arching to span a 4.75 m void without the presence of the geogrid (which allows the arching to be mobilized). Conversely, the geogrid undergoes much more deformation in the absence of the arching. Accordingly, the soil-geogrid interaction is truly a synergistic phenomenon.

In the specific case of this test, there appears to be a relationship between the fully flexible model parameters and the degree of actual arching.

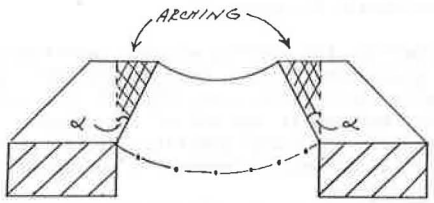

Figure 8: Schematic Representation of Arching.

Specifically, if the degree of arching is α as shown in Fig. 8, then

$$\alpha = 2(\theta_{mod} - \theta_{act})$$

where θ_{act} and θ_{mod} are respectively the actual and model deflection angles as shown in Fig. 2, and α = the angle defined by joining the top of embankment deformation point with the geogrid deformation point (Fig. 8). This relationship may be coincidental or unique to these test conditions.

When the full-interlock model was compared to the actual data, the results were quite encouraging. In the comparison, the following assumptions were made:

- gravel modulus E = 4,000 - 7,000 kPa;
- equivalent beam is 4.6 m wide (as compared to 5.5 m, which is the full embankment width); and
- equivalent beam depth is 0.85 m (as compared to 1.5 m, which is the full embankment depth), i.e., this is only the "bottom" portion of the gravel, which experiences a confining load from the gravel above.

The actual failure load bending moment (M_u) was 48 m-kN/m as compared to 54 m-kN/m predicted from the model. The model would therefore appear to be promising but requires more verification.

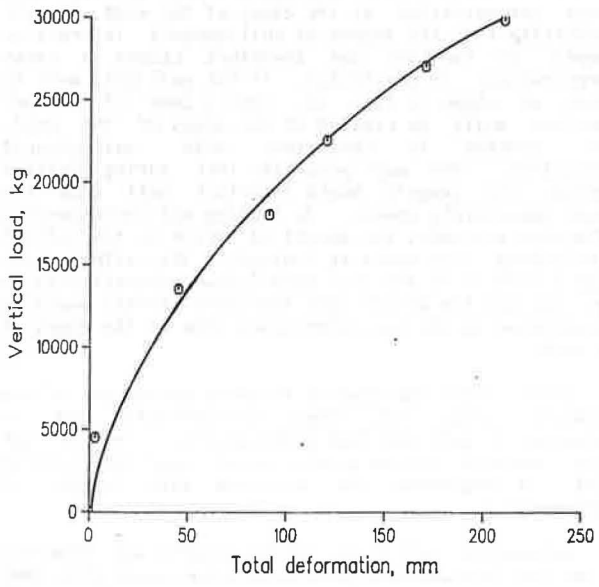

Figure 9: Total Vertical Load on Geogrid Versus Measured Elongation.

6.2 Stress-Strain Response

Considering the adverse weather conditions and the loading procedure, the instrumentation performed exceptionally well with over 70% of the electronic gauges still working at the end of the project. Through data automation, a large quantity of information was collected of which only a summary is presented here.

The localized strain information shown in Fig. 6 indicates that no strain was measured in the geogrid until the pressure in the pneumatic support system had been reduced to approximately 23 kPa.

In the load-elongation diagram shown in Fig. 9, the horizontal deformation in the geogrid was calculated using standard trigonometric arc length equations, corrected for slack in the grid and pull-out strain over the support platforms (using wire gauge information). The curve in Fig. 9 (when compared to typical stress-strain curves for the geogrid) shows that the geogrid was approaching a yield condition and probably was within 80-90% of its ultimate tensile strength.

6.3 Stress Concentrations

When the test was carried to the point of geogrid failure, the broken strands were located in the vicinity of the boundary between the edge of the support platform and the void. This apparent stress concentration at the edges of the void may have resulted from several contributing factors.

First, the geogrid may receive point loading by the stones at the edge of the void. Such loading could prove to be significant since the geogrid could be weakened, and, when the geogrid is stressed to failure, it will fail first at its weakest point. Preliminary testing on geogrid taken from the test (samples taken from platform areas) indicates a 10% loss in apparent creep strength as compared to new material.

A second possible explanation for the apparent stress concentration at the edges of the void is the possibility that the degree of soil-geogrid interaction depends on location and therefore causes a stess concentration. In particular, if the soil mass were to behave as shown in Fig. 10, then a zone of minimal interlock would be created at the edges of the void. This concept is consistent with soil-geogrid interaction. One may postulate that during initial loading, the geogrid would interlock well with the gravel immediately above. As loading and corresponding deflection proceeds, the amount of strain in the initial interlocking area would be limited. This effect would cause a "crack" in the soil mass (shown schematically in Fig. 10) and the strain (and therefore stress) would be concentrated in the non-interlocked area at the edges of the void.

Also, since the geogrid is being pulled out of the embedment area, the stress concentration may be analogous to pull-out test observations. In pull-out tests, maximum stress-strain occurs near the initial point of embedment and decreases with length of embedment.

Relaxation of stress in the geogrid was observed in certain instrumented locations, which would also tend to indicate stress transfer to other areas. The actual horizontal load in the geogrid and stress transfer will depend on the lateral earth pressure at the base of the embankment, soil-geogrid interlock, and arching in the soil. Numerical methods are currently being used to analyze the data to reach conclusions concerning stress transfer across the geogrid.

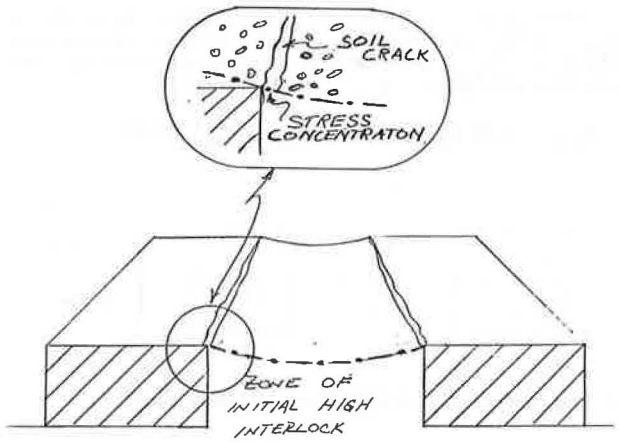

Figure 10: Schematic of Possible Stress Concentration Mechanism.

7. CONCLUSIONS

The full scale embankment test was successful and generated much useful data. The phenomenon of soil-geosynthetic synergistic interaction was verified by the test, and relationships were developed to relate this phenomenon to two different analytical models. It is not known whether these relationships have broader applications.

Although the strain-distribution data require much more analysis, the data presented in this paper showed a stress concentration near the boundary between the support platforms and the void which was spanned.

8. ACKNOWLEDGEMENTS

The authors wish to acknowledge the following for their help in preparing this paper: from GeoServices, Inc., Dr. J.F. Beech, and Ms. C. Pearce; from STS Consultants, Dr. S. Gil, Mr. C. Baker, Mr. R. Bell, Ms. C. Bonczkiewicz, and Ms. D. Moe; and from Signode, Messrs. R. Gould, D. Graffam, L. Lezon, and D. Bednarz. The authors also wish to extend their gratitude to the Signode Corporation, High Performance Plastics Division, for their extensive support as sponsors of the test.

9. REFERENCES

[1] GIROUD, J.P., "Geotextiles and Geomembranes - Definitions, Properties and Design", I.F.A.I. Publisher, (St. Paul, Minnesota, 1984), Section 2.1.

[2] KINNEY, T.C., "Field and Laboratory Study of the Use of Geotextiles to Bridge Thermokarsts", for State of Alaska Department of Transportation and Public Facilities, May, 1985, 108 pp.